Chemical Engineering Journal 151 (2009) 134–140

Contents lists available at ScienceDirect

Chemical Engineering Journal

journal homepage: www.elsevier.com/locate/cej

Optimal design and preparation of titania-supported CoPc using sol–gel for the photo-reduction of CO_2

Zhihuan Zhao*, Jimin Fan, Shaohua Liu, Zhizhong Wang

College of Chemistry and Chemical Engineering, Taiyuan University of Technology, Yinze Street, Taiyuan, 030024, China

ARTICLE INFO

Article history:
Received 3 December 2008
Received in revised form 3 February 2009
Accepted 10 February 2009

Keywords:
Sol–gel method
Photo-catalyst
CO_2 reduction
Optimization
$CoPc/TiO_2$

ABSTRACT

CoPc-loading titania ($CoPc/TiO_2$) was synthesized by an improved sol–gel method using a homogeneous hydrolysis technique. In order to increase C1 products in the photo-reduction of CO_2, preparation conditions of photo-catalysts were optimized using a four-level OAD16 (4^5) matrix in which molar ratio of reacting species, solvent, pH, mass ratio of CoPc to TiO_2, and calcining temperature were chosen as main parameters. The results obtained by orthogonal array design (OAD) method indicate that calcining temperature was the most important parameter influencing the photo-reduction of CO_2. Under optimal experimental conditions the total yield of reduction products of CO_2 in NaOH aqueous solutions was 406.65 μmol/g-catal. The grain size of $CoPc/TiO_2$ was uniform with an average diameter of approximately 11 nm. In addition, the catalyst was characterized by X-ray powder diffraction, scanning electron microscopy, UV–vis DRS, BET and FT-IR spectroscopy. $CoPc/TiO_2$ catalyst synthesized by sol–gel exhibited relatively high photochemical activity for the reduction of CO_2 compared with TiO_2 prepared by sol–gel method.

1. Introduction

Photo-reduction of CO_2 with H_2O is of significance not only in utilizing artificial photosynthesis but also in using carbon sources for the synthesis of hydrocarbons such as CH_4, HCOOH, HCHO, CH_3OH, etc. At the same time, this technology can efficiently convert solar energy into chemical energy [1]. There are a large number of studies on the CO_2 reduction to fuels using photo-catalysts [2–7], but previous work on the photo-catalytic reduction of CO_2 focused on TiO_2 and UV light irradiation. For example, Kočí et al. [7] have studied the photo-catalytic properties of TiO_2 nanoparticles on photo-reduction of CO_2. The results showed that the crystallite size plays an important role in nano-crystalline TiO_2-based photo-catalysts. As the particle size decreased, higher yields of methanol and methane over the TiO_2 nanoparticles under the illumination of UV light were obtained. However, the efficiency of this method was relatively low and an increase of yield is necessary. Tseng et al. [2] have gained methanol 4.7 μmol/g-catal. in system of TiO_2 powder and aqueous solution illuminating at 254 nm for 6 h. The quantum efficiency was 0.42%.

Apart from doping TiO_2 with a single metal or nonmetal, it is highly anticipated that doping TiO_2 with an appropriate combination of metals and/or nonmetals would, of course, result in more visible light sensitive photo-catalysts for a desired application. Li et al. [8] synthesized N–F-codoped TiO_2 photo-catalysts by spray pyrolysis (SP) using $TiCl_3$ and NH_4F precursors and observed an enhanced photo-reactivity of the materials in visible light. Luo et al. [9] prepared a Br- and Cl-codoped TiO_2 system and demonstrated the efficiency of the material for photo-catalytic splitting of water into H_2 and O_2 in the presence of Pt co-catalyst and UV light irradiation. These recent efforts and strategies have revealed that codoping TiO_2 with a metal and a nonmetal can result in the development of visible active photo-catalysts. It is well known that noble metals such as Ag, Au, and Pt possess unique electronic and catalytic properties. For example, Kim et al. [10] prepared Pt-ion-doped TiO_2, and examined its visible light activity for the photo-degradation of chlorinated organic compounds. But from an economic viewpoint, gold and platinum are very expensive and unaffordable metals for extensive use in photo-catalysis. Compared to gold and platinum, silver is a more affordable metal and deserves further investigation.

More recently, an optical-fiber reactor is employed to photo-catalytically reduce CO_2 with H_2O to fuels under UVA artificial light and concentrated natural sunlight [11,12]. The optical fiber is coated with gel-derived TiO_2–SiO_2 mixed oxide-based photo-catalysts. Fe atom is found to be inserted into the TiO_2–SiO_2 lattice during sol–gel process, resulting in the full visible light absorption as well as the effect on product selectivity of the derived catalyst. Under UVA, ethylene is mainly produced on Cu–Fe/TiO_2 catalyst with the quantum yield of 0.0235%, whereas Cu–Fe/TiO_2–SiO_2 catalyst is observed to favor methane production with the quantum yield of 0.05%. There is only methane evolved over both bare TiO_2–SiO_2 and

---

* Corresponding author. Tel.: +86 351 8350665; fax: +86 351 6018701.
E-mail address: zzh1972129@163.com (Z. Zhao).

1385-8947/$ – see front matter © 2009 Elsevier B.V. All rights reserved.
doi:10.1016/j.cej.2009.02.005

Cu–Fe/TiO_2–SiO_2 catalysts under natural sunlight with the production rates of 0.177 and 0.279 mmol/g-catal. h, respectively.

Consequently, higher performance in visible photo-catalysis is strongly required for future wide applications. Key technology will be surface modification for a higher sensitivity. Many types of supported photo-catalytic TiO_2 continue to be the subject of extensive development worldwide [13]. Besides industrial production and practical use of the new photo-catalytic materials, there is an increasing need for a simple and reliable procedure to produce visible light photo-catalyst. So in this paper we will produce the efficient photo-catalyst in the heuristic of Siviero et al. [14] hybrid gas sensing devices based on ZnPc and nano-structured titania. The enlargement of the organic–inorganic interface region using a three-layer architecture gives rise to a strong enhancement of the performances of the hybrid sensors. It prompts us to hybrid MPc and titania together.

In this work, a simple method for preparing highly active titania and titania-supported CoPc (cobalt phthalocyanine) nanoparticles (CoPc/TiO_2) for photo-catalysis was developed, which includes a modified sol–gel procedure based on esterification reaction. Moreover, a preferable production was obtained when they were used for photo-reduction of CO_2 in NaOH aqueous solution. Hydrolysis of titanium compounds, such as titanium alkoxide and halide, has been widely adopted to prepare TiO_2 nanoparticles [15–19]. However, the high hydrolytic reactivity of titanium alkoxide and halide may cause some uncontrolled precipitation, thus resulting in the losses of material [15].

To improve the efficiency of photo-reduction of CO_2, photo-catalysts should be optimized. However, various parameters in preparation, such as molar ratio of raw material, solvent, pH, mass ratio of CoPc to TiO_2 and calcining temperature, potentially affect the characteristics of photo-catalysts and consequently their photo-catalytic activity. The optimization of preparation conditions represents a critical step in the development of a novel sol–gel method. Orthogonal array design (OAD) is a very useful type of factorial design [20–22]. The results of OAD experiments can be treated by analysis of variance and/or direct observation analysis (also called range analysis) [23].

The objectives of this work are: (1) to suggest a method for the synthesis of anatase TiO_2 and CoPc/TiO_2 nanoparticles by using sol–gel method, (2) to apply orthogonal array design method for the optimization of catalyst performance and to obtain the TiO_2 and CoPc/TiO_2 nanoparticles with narrow particle size distribution under optimal synthesis conditions, and (3) to evaluate the effect of several principal parameters influencing the photo-reduction of CO_2 with H_2O.

2. Experimental procedure

2.1. Preparation and characterization of catalysts

Degussa P-25 TiO_2 was commercially available, which was a mixture of 75% anatase and 25% rutile. Its BET surface area was about 50 $m^2\,g^{-1}$. Other chemicals titanium(IV) butoxide, anhydrous ethanol, acetic acid and hydrochloric acid were reagent grade quality and were used without further purification. CoPc was commerced from Tokyo Chemical Industry Co., Ltd., w(CoPc) = 98%. All aqueous solutions were made up in deionized and doubly distilled water.

Catalysts were prepared at ambient temperature by sol–gel method, as illustrated in Fig. 1. The precursor was titanium(IV) butoxide ($Ti(OC_4H_9)_4$, 97%). $Ti(OC_4H_9)_4$ was dissolved in anhydrous ethanol, and then mixed with acetic acid, hydrochloric acid and deionized water under stirring. To avoid rapid precipitation during polycondensation and formation of unstable colloidal sols, the hydrolyzing water was homogeneously released by the esterification of ethanol and acetic acid [24].

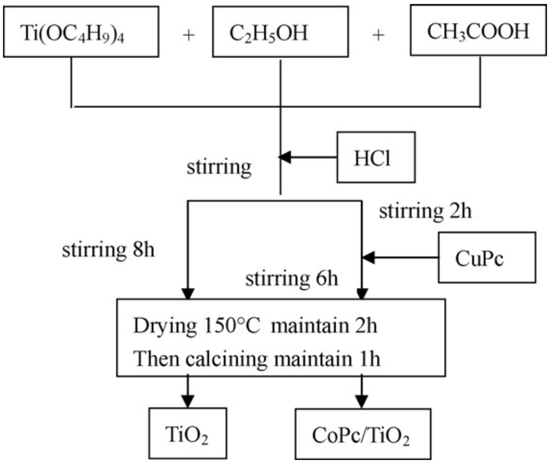

Fig. 1. Procedure of catalyst preparation.

The clear solution was stabilized by stirring at ambient temperature for 8 h, then placed and aged for 24 h. Subsequently the transparent sol was dried at 150 °C, and then calcined to burn off hydrocarbons. The sample was crushed into powder in a mortar at last.

The amorphous state of the photo-catalysts was confirmed by X-ray diffraction (XRD) recorded on a Rigaku 2304 diffractometer with Ni-filtered Cu Kα radiation. A diffusive reflective UV–vis spectrophotometer (DRS) was employed to measure the UV–vis absorption and estimate the bandgap of the catalysts. Scanning electron microscopy (SEM) was used to characterize the morphology of catalysts. The specific surface area and pore size distribution of catalysts were measured by N_2 adsorption in a Thermo Electron Corporation Sorptomatic 1990. FT-IR spectra of the solid catalysts are recorded on a Perkin-Elmer FT-IR1760 spectrometer and use the potassium bromide (KBr) pellet technique.

2.2. Photo-catalytic reaction

Photo-catalytic reaction was carried out in a Pyrex cell with an optical window (volume of solution was 100 ml). Catalyst concentration was 100 g/l in 100 ml of 0.1N NaOH aqueous solution. Illumination was performed with a 500 W tungsten-halogen lamp. The reactor was tightly closed during reaction and stirred continuously by a magnetic stirring bar to prevent sedimentation of catalyst, then CO_2 was bubbled through the reactor for at least 30 min to purge air and to saturate the solution. The yields for the formation of methanol, formaldehyde and formic acid were determined with UV–vis spectrophotometer. Gaseous products were analyzed in a GC equipped with thermal conductivity detection and a 2 m carbon molecular sieve column.

Blank reaction was conducted to ensure that hydrocarbon production was due to the photo-reduction of CO_2 and to eliminate surrounding interference. The conditions for three blank tests are: (1) vis-illumination, no catalyst, CO_2; (2) dark, catalyst, CO_2; and (3) vis-illumination, catalyst, N_2. No product was detected in the above three blank tests.

2.3. Orthogonal array design and selection of variables

On the basis of numerous literatures and our previous work, significant factors were identified, and the most significant factors were chosen for optimization, using a four-level OAD with an OA16 (4^5) matrix. The possible interactions between variables were not

Table 1
Parameters and levels used in preparing of CoPc/TiO_2.

	Variants/factors	Level 1	Level 2	Level 3	Level 4
A	Molar ratio of $Ti(OC_4H_9)_4/C_2H_5OH/CH_3COOH/H_2O$	1:2:1:1	1:4:2:2	1:6:3:3	1:8:4:0
B	Solvent	No	CH_2Cl_2	DMF	Toluene
C	Hydrochloric acid (ml)	0.25	0.50	0.75	1.00
D	Mass ratio of CoPc/TiO_2 (%)	0.50	1.00	2.00	3.00
E	Calcining temperature (°C)	300	400	500	600

incorporated in the matrix, and focus was placed on the main effects of the four most important factors. For successful preparation of photo-catalysts, several factors were taken into consideration prior to the experiments as following:

- *Molar ratio of reacting species*: denoting $Ti(OC_4H_9)_4$:C_2H_5OH:CH_3COOH:H_2O. The hydrolyzing water was homogeneously released by the esterification of ethanol and acetic acid and a little additional water was added, which provided a superior condition for the nucleation and growth of the primary particles in solution.
- *Solvent*: toluene, dichloromethane (CH_2Cl_2), dimethyl formamide (DMF). In this study, several solvents were selected to dissolve more CoPc into the transparent sol and make some significant influence on the structure and photo-catalytic activity of TiO_2 nanoparticles. Of course the use of organic solvents was restricted to prevent pollution and waste so CoPc also was added immediately into sol without solvent.
- *pH*: the addition of concentrated hydrochloric acid was to promote hydrolyzation and restrain agglomeration of sol by providing sol with positive charges. Its quantity varied from 0 to 1 ml.
- *Mass ratio of CoPc to TiO_2*: this value influenced the efficiency of photo-reduction of CO_2.
- *Calcining temperature*: a great deal of study showed that anatase had higher catalytic activity than rutile and amorphous TiO_2. Therefore, calcining temperature determined whether anatase could be formed or not.

Each factor was tested at four levels covering a broad range (Table 1).

3. Results and discussion

3.1. Analysis of experimental data

The orthogonal array of L_{16} type was used and represented in Table 2. Five four-level parameters are positioned in a L_{16} orthogonal array table. The numbers 1, 2, 3 and 4 in Table 2 denote the four levels of the factor, respectively, as listed in Table 1.

Table 2
Results of OA16 (4^5) experimental design for the photo-catalytic reduction of CO_2.

Experiment no.	A	B	C	D	E	Total products (μmol/g-catal.)
1	1	1	1	1	1	251.47
2	1	2	2	2	2	299.90
3	1	3	3	3	3	158.27
4	1	4	4	4	4	157.49
5	2	1	2	3	4	261.36
6	2	2	1	4	3	208.41
7	2	3	4	1	2	262.43
8	2	4	3	2	1	174.50
9	3	1	3	4	2	281.62
10	3	2	4	3	1	153.93
11	3	3	1	2	4	164.85
12	3	4	2	1	3	223.86
13	4	1	4	2	3	241.95
14	4	2	3	1	4	214.92
15	4	3	2	4	1	165.58
16	4	4	1	3	2	289.84

The total products of the photo-catalytic reduction of CO_2 for the parameters at different levels are shown in Table 3. The maximum–minimum value for calcining temperature is the highest value. Therefore, it can be concluded that calcining temperature of photo-catalysts is the most significant parameter affecting CO_2 reduction.

Fig. 2 shows the effect of different parameters on the photo-catalytic reduction of CO_2. Each value was an average of three measurements, in each of which the parameter of interest was kept constant, and the other parameters were varied.

Fig. 2 and Table 3 indicate that preferable conditions for preparing titania-supported CoPc using sol–gel for the photo-reduction of CO_2 were: molar ratio of raw materials: 1:4:2:2; no solvent; 0.5 ml hydrochloric acid; mass ratio of CoPc to TiO_2 0.50%; and calcining temperature 400 °C. On the other hand, it can be seen that the five factors influenced the photo-reduction of CO_2 in a descending order of calcining temperature, solvent, hydrochloric acid, mass ratio of CoPc to TiO_2, and molar ratio of raw materials. Further experiments under optimized conditions show that yield of 400 μmol/g-catal. was obtained in NaOH aqueous solutions, which greatly exceeded that of in Table 2. Interaction of different parameters has not been considered in this study. It needs further studies in next work.

In order to evaluate the effect of calcining temperature on the photo-reduction of CO_2 with H_2O, one-variable-at-a-time method was used in experiment. The results were demonstrated in Fig. 3. Calcining temperature varied from 300 to 800 °C while other conditions were kept constant as preferable conditions.

From Fig. 3, it can be seen that total product of CoPc/TiO_2 calcined at 400 °C reached its maximum, in agreement with the previous results obtained from direct observation analysis. The reason is that the catalyst had relatively rich and uniform crystalline phase, as can be seen from XRD measurement. The photo-catalytic activity of sample calcined at 300 °C was lowest of all. This is due to the

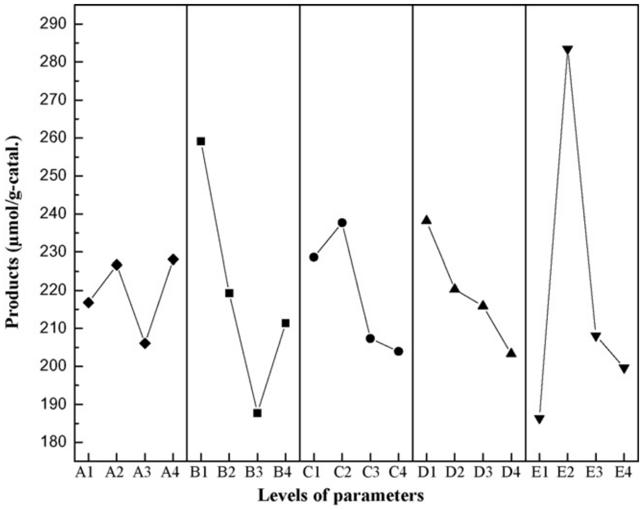

Fig. 2. Effect of different parameters on the photo-catalytic reduction of CO_2.

Table 3
Total products of the photo-catalytic reduction of CO_2 at different parameter level.

Symbol	Parameter	Total products (μmol/g-catal.)				
		Level 1	Level 2	Level 3	Level 4	Maximum–minimum
A	Molar ratio of $Ti(OC_4H_9)_4/C_2H_5OH/CH_3COOH/H_2O$	216.782	226.675	206.065	228.072	22.007
B	Solvent	259.100	219.290	187.783	211.423	71.317
C	Hydrochloric acid (ml)	228.642	237.675	207.327	203.950	33.725
D	Mass ratio of $CoPc/TiO_2$ (%)	238.170	220.300	215.850	203.275	34.895
E	Calcining temperature (°C)	186.370	283.447	208.123	109.655	173.792

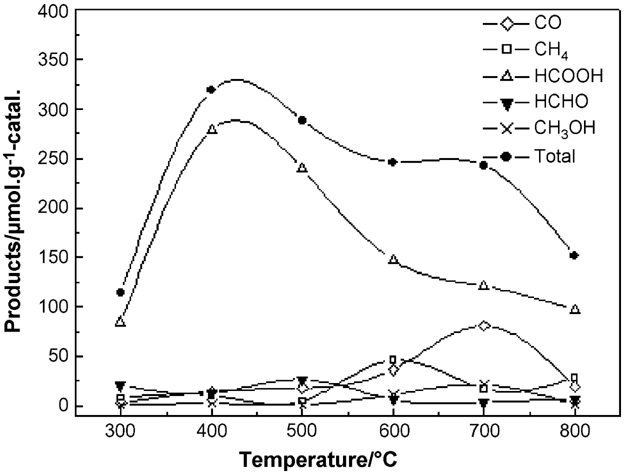

Fig. 3. Effect of calcining temperature on the efficiency of production.

presence of relatively poor crystalline phase and some impurities, such as acetates, which was not eliminated completely from samples. With the increase of the temperature, amorphous TiO_2 was transformed into anatase, which is well known as a photo-catalyst of high photo-activity. When the temperature was increased to 500 or 600 °C, anatase was partly transformed into rutile. Generally, the composite of two phases might be benefit to the separation of photo-generated electrons and holes, thus resulting in high photo-catalytic activity [25]. Because of photo-catalytic activity strongly depends on the lifetime of the electron–hole pairs generated by photo-excitation. As the recombination probability is decreased, the life is prolonged and results in a high photo-catalytic activity in anatase. As shown in Table 4, the catalysts calcined at 500 and 600 °C represent higher photo-catalytic activity than those obtained at 700 and 800 °C's, because the latter ones contained more rutile with bigger crystallite size and smaller S_{BET}.

As calcining temperature increased, more and more TiO_2 in $CoPc/TiO_2$ was transformed into rutiles, and correspondingly, anatase decreased. Table 4 indicates that in $CoPc/TiO_2$ catalysts more TiO_2 was converted into rutile at 400 °C than in sol–gel TiO_2, suggesting that the dispersion of CoPc in TiO_2 lattice induced the decrease of phase transfer temperature from anatase to rutile. This may be the disfigurement of CoPc into sol–gel TiO_2 which was more profitable for rutile phase to grow than anatase.

Table 4
Particle size distribution of catalysts calcining of different temperatures.

Catalyst	Particle size[a] (nm)	Content of rutile[b] (%)	Yield[c] (μmol/g-catal.)
0.5% $CoPc/TiO_2$ (400 °C[d])	11.02	27.57	341.74
0.5% $CoPc/TiO_2$ (500 °C)	12.57	29.75	263.33
0.5% $CoPc/TiO_2$ (600 °C)	17.56	77.98	226.55
0.5% $CoPc/TiO_2$ (700 °C)	18.78	90.67	225.94
0.5% $CoPc/TiO_2$ (800 °C)	18.04	84.51	130.06
TiO_2 (400 °C)	11.33	18.73	200.02

[a] Estimated from FWHM of XRD by Scherrer equation.

[b] Calculated from relative peak intensity of anatase and rutile.

[c] Conditions of reaction: irradiation time 6 h, 0.1 mol/l sodium hydroxide100 ml, catalyst 150 mg.

[d] Calcining temperature of catalysts.

The effect of irradiation time on the formation of photo-reduced products was investigated over a period of 6–50 h, as were illustrated in Fig. 4. The total yield in CO_2-saturated system increased rapidly with the photolysis time at early stage, as more photo-electrons were generated with increasing time of light exposure. After 20 h of irradiation, the total yield flattened out. Similar trends were also observed for HCOOH and CO. This can be attributed to the saturation of the adsorption sites on the surface of TiO_2 with intermediate products. The yield of formaldehyde continued to decrease after 20 h due to its consumption as an intermediate product. At the same time, the yield of CH_4 and CH_3OH continued to increase to some extent because CH_4 and CH_3OH, as the ultimate reducing species in the photo-catalytic reduction of CO_2, were not be consumed.

From the above results and literature reports, a reaction scheme for the photo-catalytic reduction of carbon dioxide in NaOH solution is proposed as follows. Photo-excited electrons (e^-) and positive holes (h^+) are produced when incident photons are absorbed in $CoPc/TiO_2$ and then transfer to TiO_2 and CoPc, respectively (Eqs. (1) and (2)). Therefore, the photo-excited electrons and holes in the lattices are separated and trapped by appropriate sites of $CoPc/TiO_2$ to avoid recombination. CO_2 molecules adsorbed on the surface of TiO_2 gain electrons and are reduced to CO, CH_4, HCOOH, HCHO, CH_3OH, and so on. Furthermore, the interaction of CO_2 molecules with the excited state of $CoPc^*/TiO_2$ leads to the formation of $CO_2^{\bullet -}$ anion radicals (Eq. (3)), which are reduced further to $HCOO^-$ or CO (Eqs. (4)–(6)). Then the predominant $HCOO^-$ in the solution can be further transformed into HCHO and CH_3OH, as shown in Eq. (7) and (8).

$$\mathrm{CoPc}(S_0) + h\nu \rightarrow \mathrm{CoPc} * (S_1) \tag{1}$$

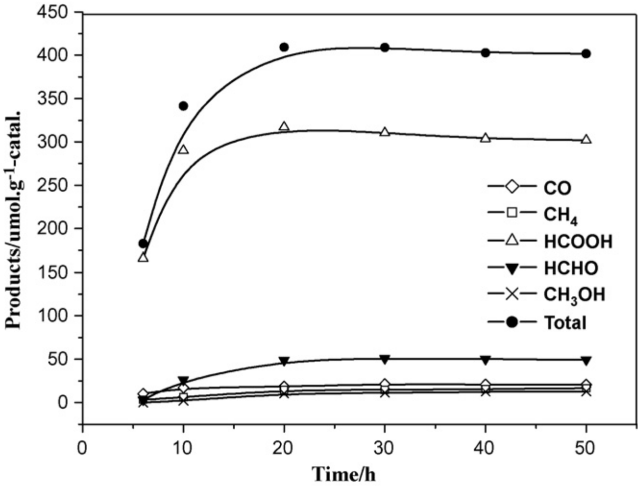

Fig. 4. Influence of irradiation time on the photo-catalytic reduction of CO_2.

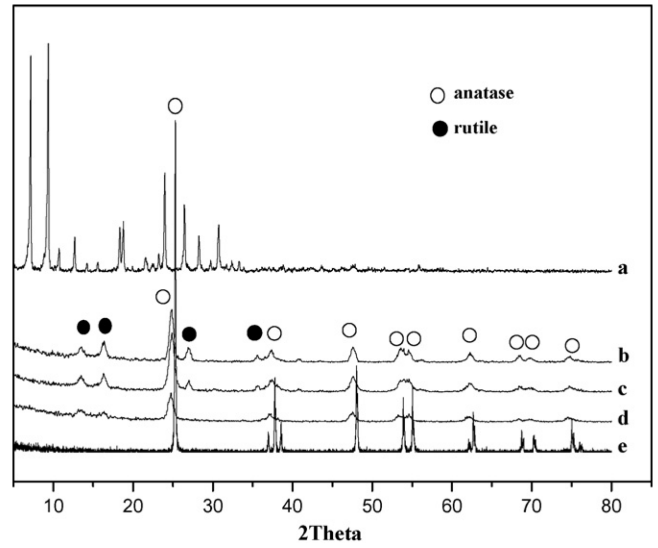

Fig. 5. XRD patterns of TiO_2 and $CoPc/TiO_2$. (a) CoPc; (b) 1.0 wt.% $CoPc/TiO_2$; (c) 0.5 wt.% $CoPc/TiO_2$; (d) TiO_2 (this work); (e) P-25.

$$CoPc*(S_1) + TiO_2(CB) \rightarrow h^+(CoPc/VB) + e^-(TiO_2/CB) \tag{2}$$

$$CO_2 + e^- \rightarrow CO_2{}^{\bullet -}(ad) \tag{3}$$

$$CO_2{}^{\bullet -}(ad) + H^+ + e^- \rightarrow HCOO^- \tag{4}$$

$$CO_2{}^{\bullet -}(ad) + H^+ + e^- \rightarrow CO + OH^- \tag{5}$$

$$\text{or}CO_2{}^{\bullet -}(ad) + CO_2 + e^- \rightarrow CO + CO_3{}^{2-} \tag{6}$$

$$HCOO^- + 2H^+ + 2e^- \rightarrow HCHO \tag{7}$$

$$HCHO + 2H^+ + 2e^- \rightarrow CH_3OH \tag{8}$$

3.2. Characterization of $CoPc/TiO_2$

The crystallinity of the prepared samples was examined by XRD analysis. The XRD patterns in Fig. 5 verify that the samples were mainly crystallized to anatase phase and had a small quantity of rutile by calcinations. The peaks at 2θ values of 24.88, 37.42, 47.66, 53.49, 54.51, 62.29, 68.55, 69.97 and 74.69° were identified by comparison with literature data and attributed to the (1 0 1), (0 0 4), (2 0 0), (1 0 5), (2 1 1), (2 0 4), (1 1 6), (2 2 0) and (2 1 5), respectively, of polycrystalline with an anatase structure. It is noteworthy that the diffractograms of the samples $CoPc/TiO_2$ (b, c) do not present signals of CoPc. The absence of CoPc peaks could be attributed to the complete dispersion of CoPc into TiO_2 in the form of molecule or very fine crystal when CoPc was added along with the hydrolysis of titanium butoxide at low loading quantity. It is possible that some of CoPc was enveloped by TiO_2 particles.

The structural parameters of catalysts were given in Table 5. The results showed that while CoPc was doped, the specific surface area of xerogel 0.5% $CoPc/TiO_2$ was 90.7 m^2/g and the pore volume was 0.1377 cm^3/g. For 0.5% $CoPc/TiO_2$, its pore size (2.52 nm) was larger than that of CoPc molecule (1.6 nm). Therefore, the encapsulation of CoPc molecules in varied nanometer "cage" prevented them from colliding with each other. So these "cage" suppressed dimerization of CoPc and improving the productivity of reduction CO_2.

Table 5
Structural parameters of catalysts.

Catalyst	S_{BET} (m^2/g)	Pore volume (cm^3/g)	Pore size radius (Å)
TiO_2	84.3	0.2133	40.3
0.5% $CoPc/TiO_2$ (400 °C)	90.7	0.1377	25.2
1.0% $CoPc/TiO_2$ (400 °C)	75.6	0.2025	39.2

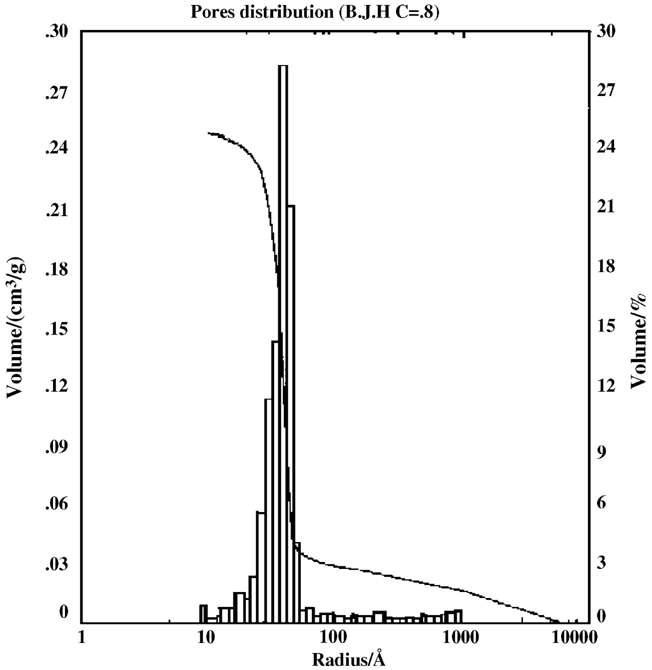

Fig. 6. Pore size distribution of 1.0% $CoPc/TiO_2$.

The pore size of the sol prepared by doping CoPc under the Co/Ti mass ratio of 1.0 was narrowly distributed around 11 nm. After calcination at 400 °C, the pore size of the xerogel was also very uniform and the mean pore diameter was about 3.92 nm, as can be seen from Fig. 6.

SEM was used to investigate the microstructure of $CoPc/TiO_2$. As shown in Fig. 7, the size of crystallites was 11–18 nm, very close to that obtained by XRD analysis (Table 4). The crystallites were a little aggregated, which decreased the S_{BET} of samples. The aggregation may be promoted by the burning-off of residue acetates and sulfates during calcination.

Diffusive reflectance UV–vis spectroscopy was employed to determine the light-absorbing scope of CoPc species on the TiO_2 samples. MPc usually exhibit strong electronic transition in visible and near-infrared range, both because of $\pi \rightarrow \pi^*$ transition. The Q band at 600–800 nm is regarded as the characteristic absorption

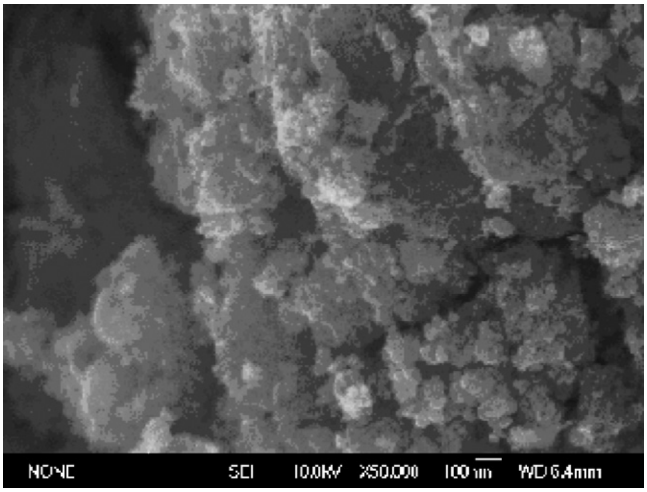

Fig. 7. SEM image of 0.5% $CoPc/TiO_2$.

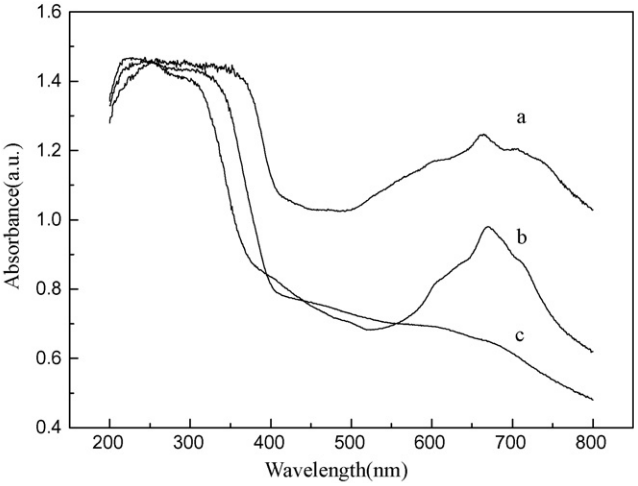

Fig. 8. DRS spectra of dried CoPc/TiO_2. (a) 3.0% CoPc/TiO_2; (b) 1.0% CoPc/TiO_2; (c) 0.5% CoPc/TiO_2.

band. Fig. 8 was the DRS spectra of dried gel. The molecular MPc in the matrix usually exists in three kinds of state: monomer, dimmer and aggregate. In Fig. 8 the absorption bands of 670 nm and a weak absorption band around 610 nm were attributed to monomer CoPc, while the red-shifted band around 700 nm was attributed to CoPc aggregate [26].

In Fig. 8, the strong bands observed from 600 to 800 nm indicate the existence of CoPc species on the surface of TiO_2. Moreover, the absorption edge was shifted to longer wavelengths with increasing CoPc content. So the loading of CoPc on surface of TiO_2 expanded adsorption of visible light, which is favorable for photo-catalytic reaction.

The FT-IR spectra of CoPc, TiO_2 and 3.0 wt.% CoPc/TiO_2 samples are shown in Fig. 9. In curve (c) the 750 cm^{-1} band was assigned to the vibration of Pc ring, 1086 cm^{-1} to the macrocyclic ring's C–C stretching, 1164 cm^{-1} to the pyrrole ring's C–H stretching, 1333 cm^{-1} to the isoindoline ring's C–C stretching, 1426 cm^{-1} to the pyrrole ring's C–C stretching, and 1503 and 1605 cm^{-1} to the C=C and C=N stretching, respectively. The moderate intensity absorption band at 888–919 cm^{-1} was assigned to the metal–ligand vibration. Pure TiO_2 (curve (b)) exhibited OH bending and stretching of water at 1600 cm^{-1}. In addition, a weak band at 1340 cm^{-1} corresponded to Ti–O–Ti vibration.

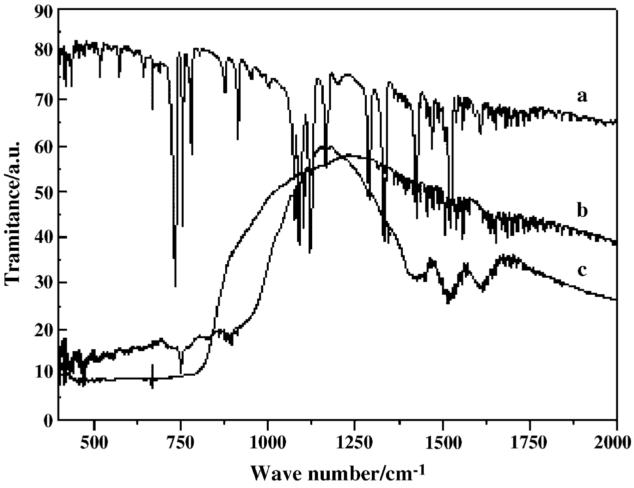

Fig. 9. IR spectra of catalysts. (a) CoPc; (b) TiO_2; (c) 3.0 wt.% CoPc/TiO_2.

Comparing curves (a) and (c), the consistency in the main absorption bands of the CoPc/TiO_2 confirms along with DRS measurements, and successful support of CoPc in the matrix of TiO_2.

4. Conclusions

Nano-sized CoPc/TiO_2 particles were synthesized by a novel sol–gel method for the photo-reduction of CO_2 in visible light. The grain size of CoPc/TiO_2 was narrowly distributed around 11 nm. In the experiment it can be seen that the composite of two phases is benefit to the separation of photo-generated electrons and holes, thus resulting in high photo-catalytic activity. So in this study dispersion of CoPc in TiO_2 lattice induced the decrease of phase transfer temperature from anatase to rutile. CoPc is completely dispersed into TiO_2 lattice. At the same time, the absorption edge of photo-catalyst was shifted to longer wavelengths with increasing CoPc content. So the loading of CoPc on surface of TiO_2 expanded adsorption of visible light, which is favorable for photo-catalytic reaction.

Orthogonal array design was used to optimize the parameters for preparing the photo-catalysts. Various factors affecting the particle size and efficiency of CO_2 reduction were analyzed. As a result, the calcining temperature of catalysts was found to be the most significant parameter. The optimized conditions were determined as: molar ratio of raw materials: 1:4:2:2; no solvent; 0.5 ml hydrochloric acid; mass ratio of CoPc to TiO_2 0.50%; and calcining temperature 400 °C, which gave the total yield of CO_2 in NaOH aqueous solutions 406.65 μmol/g-catal. The total yield in CO_2-saturated system increased rapidly with the photolysis time at early stage. After 20 h of irradiation, the total yield, HCOOH and CO flattened out. The yield of formaldehyde continued to decrease after 20 h due to its consumption as an intermediate product. At the same time, the yield of CH_4 and CH_3OH continued to increase to some extent because CH_4 and CH_3OH, as the ultimate reducing species in the photo-catalytic reduction of CO_2, were not be consumed.

Experimental results demonstrate that CoPc/TiO_2 catalyst synthesized in this study exhibited relatively high photochemical activity for the reduction of CO_2. The distribution of CoPc on TiO_2 particles is critical to maximize the yield of reduction products. CoPc can be promoted by visible light to produce electron–hole pairs. In this study, the catalytic reduction CO_2 has great advantage over green plants of not having to support a living system. The transformation of photo to chemical energy by a non-living catalyst should be more efficient than by a life-supporting one. Ideally, this technology provides a probability to reduce CO_2 in aqueous under solar irradiation. Visible light photo-catalysts applicable to practical use were discovered quite recently. We sincerely hope for a further progress of research and development of visible light photo-catalysts.

Acknowledgement

This work was financially supported by the Natural Science Funds (no. 2008021015) of China Shanxi Province.

References

[1] G.R. Dey, A.D. Belapurkar, K. Kishore, Photo-catalytic reduction of carbon dioxide to methane using TiO_2 as suspension in water, J. Photochem. Photobiol. A: Chem. 163 (2004) 503–508.
[2] I.-H. Tseng, W.-C. Chang, J.C.S. Wu, Photoreduction of CO_2 using sol–gel derived titania and titania-supported copper catalysts, Appl. Catal. B: Environ. 379 (2002) 37–48.
[3] I.-H. Tseng, J.C.S. Wu, Chemical states of metal-loaded titania in the photoreduction of CO_2, Catal. Today 97 (2004) 113–119.
[4] A.V. Lobanov, S.N. Kholuiskaya, G.G. Komissarov, Photocatalytic synthesis of formaldehyde from CO_2 and H_2O_2, Doklady Phys. Chem. 399 (2004) 266–268.

[5] Y. Shioya, K. Ikeue, M. Ogawa, M. Anpo, Synthesis of transparent Ti-containing mesoporous silica thin film materials and their unique photocatalytic activity for the reduction of CO_2 with H_2O, Appl. Catal. A: Gen. 254 (2003) 251–259.

[6] J.C.S. Wu, H.-M. Lin, C.-L. Lai, Photo reduction of CO_2 to methanol using optical-fiber photoreactor, Appl. Catal. A: Gen. 296 (2005) 194–200.

[7] K. Kočí, L. Obalová, L. Matějová, D. Plachá, J. Jirkovský, O. Šolcová, Effect of TiO_2 particle size on the photocatalytic reduction of CO_2, Appl. Catal. B: Environ., in press.

[8] D. Li, H. Haneda, S. Hishita, N. Ohashi, Visible-light-driven N–F-codoped TiO_2 photocatalysts. 1. Synthesis by spray pyrolysis and surface characterization, Chem. Mater. 17 (2005) 2588–2595.

[9] H. Luo, T. Takata, Y. Lee, J. Zhao, K. Domen, Y. Yan, Photocatalytic activity enhancing for titanium dioxide by co-doping with bromine and chlorine, Chem. Mater. 16 (2004) 846–849.

[10] S. Kim, S.-J. Hwang, W. Choi, Visible light active platinium-ion-doped TiO_2 photocatalyst, J. Phys. Chem. B 109 (2005) 24260–24267.

[11] N. Thevinh, J.C.S. Wu, Photoreduction of CO_2 in an optical-fiber photoreactor: effects of metals addition and catalyst carrier, Appl. Catal. A: Gen. 335 (2008) 112–120.

[12] N. Thevinh, J.C.S. Wu, Photoreduction of CO_2 to fuels under sunlight using optical-fiber reactor, Solar Energy Mater. Solar Cells 92 (2008) 864–872.

[13] Urh Cernigoj, Urska Lavrencic Stangara, Polonca Trebsea, Mohamed Sarakhab, Determination of catalytic properties of TiO_2 coatings using aqueous solution of coumarin: standardization efforts, J. Photochem. Photobiol. A: Chem. 201 (2009) 142–150.

[14] F. Siviero, N. Coppede, A.M. Taurino, T. Toccoli, P. Siciliano, S. Iannotta, Hybrid titania–zincphthalocyanine nanostructured multilayers with novel gas sensing properties, Sens. Actuators B 130 (2008) 405–410.

[15] M. Ivanda, S. Music, S. Popovic, M. Gotic, XRD, Raman and FT-IR spectroscopic observations of nanosized TiO_2 synthesized by the sol–gel method based on an esterification reaction, J. Mol. Struct. 480/481 (1999) 645–649.

[16] V Nguyen, J.C.S. Wu, Photoreduction of CO_2 to fuels under sunlight using optical-fiber reactor, Solar Energy Mater. Solar Cells 92 (2008) 864–872.

[17] C. Wang, Z.-X. Deng, Y. Li, The synthesis of nanocrystalline anatase and rutile titania in mixed organic media, Inorg. Chem. 40 (2001) 5210–5214.

[18] I.-H. Tseng, J.C.S. Wu, H.-Y. Chou, Effects of sol–gel procedures on the photocatalysis of Cu/TiO_2 in CO_2 photoreduction, J. Catal. 221 (2004) 432–440.

[19] W. Liu, A.-P. Chen, J.-P. Lin, Z.-M. Dai, W. Qiu, W. Liu, M.-Q. Zhu, S. Usuda, Preparation of controllable crystalline nano-TiO_2 by homogeneous hydrolysis, Chem. Lett. (2004) 390–391.

[20] G. Tauguchi, System of Experimental Design, vols. 1 and 2, Krus International, New York, NY, 1986.

[21] P. Billot, B. Pitard, Taguchi design experiments for optimizing the gas chromatographic analysis of residual solvents in bulk pharmaceuticals, J. Chromatogr. 623 (1992) 305–313.

[22] H.B. Wan, W.G. Lan, M.K. Wong, C.Y. Mok, Orthogonal array designs for the optimization of liquid chromatographic analysis of pesticides, Anal. Chim. Acta 289 (1994) 371–380.

[23] G. Zhu, H. Ju, Determination of naproxen with solid substrate room temperature phosphorimetry based on an orthogonal array design, Anal. Chim. Acta 506 (2004) 177–181.

[24] J.C.-S. Wu, L.-C. Cheng, An improved synthesis of ultrafiltration zirconia membranes via the sol–gel route using alkoxide precursor, J. Membr. Sci. 167 (2) (2000) 253–261.

[25] J.C. Yu, J. Yu, W. Ho, L. Zhang, Preparation of highly photocatalytic active nano-sized TiO_2 particles *via* ultrasonic irradiatio, Chem. Commun. (2001) 1942–1943.

[26] Hongbing Zhan, Minquan Wang, Wenzhe Chen, In situ synthesis of metallophthalocyanines in inorganic matrix, Mater. Lett. 55 (2000) 97–103.